Supporting Information

Receptor-Independent Transfer of Low Density Lipoprotein Cargo to Biomembranes

Markus Axmann[1], *Erdinc Sezgin*[2], *Andreas Karner*[3], *Jiri Novacek*[4], *Michael D. Brodesser*[3], *Clemens Röhrl*[1], *Johannes Preiner*[3], *Herbert Stangl*[1] *& Birgit Plochberger*[3*]

[1] Medical University of Vienna, Center for Pathobiochemistry and Genetics, Institute of Medical Chemistry, Vienna, 1090, Austria

[2] MRC Human Immunology Unit, Weatherall Institute of Molecular Medicine, University of Oxford, Oxford, OX3 9DS, UK

[3] Upper Austria University of Applied Sciences, Campus Linz, Garnisonstrasse 21, 4020 Linz, Austria

[4] CEITEC, Masaryk University, University Campus Bohunice, Brno, 62500, Czech Republic

[*]Correspondence: *birgit.plochberger@fh-linz.at* & *herbert.stangl@meduniwien.ac.at*

KEYWORDS

Low Density Lipoprotein, (High-Speed) Atomic Force Microscopy, Fluorescence (Cross) Correlation Spectroscopy, Single-molecule-sensitive imaging, cryo-Electron Microscopy, Cholesterol transfer

EXPERIMENTAL METHODS

Reagents: Atto647N NHS-ester was obtained from Attotec. Sephadex G-25 fine resin, egg PhosphatidylCholine (PC), cholesteryl oleate, sodium cyanoborohydride ($NaCNBH_3$), triethylamine (TEA), 3-AminoPropyl-TriEthoxySilan (APTES), EThanolAmine (ETA), sodium deoxycholate, sucrose, glucose and HEPES were from Sigma. 1,2-DiOleoyl-sn-glycero-3-PhosphoCholine (DOPC) was purchased from Avanti Polar Lipids. Cholesterol linked to BodipyFL (TopFluor-Cholesterol, C-BodipyFL) was obtained from Avanti Polar Lipids, C-Laurdan [1] was purchased from 2pprobes (2pprobes.com).

Cells: Cells from the Chinese Hamster Ovary (CHO) cell line CHOK1 were maintained in Dulbecco's modified Eagle Medium/Nutrient Mixture F-12 (Sigma Aldrich) supplemented with Penicillin/Streptomycin (100 U/ml and 0.1 mg/ml final concentration, Sigma Aldrich), 2 mM L-Glutamine (Roth) and 10% Fetal Calf Serum (FCS, Sigma Aldrich).

Lipoprotein Particle Isolation and Labeling: LDL particles were isolated from plasma, obtained from normo-lipidemic healthy volunteers, as previously described [2]. Blood donations were approved by the Ethics Committee, Medical University of Vienna (EK-Nr. 511/2007, EK-Nr. 1414/2016). Its proteins were covalently linked to Atto647N at pH=8.3 according to the manufacturer's instruction. Cholesterol-BodipyFL was incorporated into the lipid leaflet of LDL particles via incubation at 37 °C for 2 h. Free dye and excessive cholesterol was removed via extensive dialysis.

Tip-Chemistry: Commercially available Silicon cantilevers (MSNL-10, Veeco Instruments NY) were amine-functionalized via gas-phase silanization with AminoPropyl-TriEthoxySilane (APTES) as described [3]. A heterobifunctional (aldehyde-NHS) linker was prepared as described in [4] but without the PolyEthylene Glycol (PEG) moiety. 3.3 mg of the linker were dissolved in 0.5 mL chloroform and transferred into a small glass reaction chamber. 30 µL of triethylamine was added, and the ethanolamine-coated tips were immediately submerged for 2 h. Subsequently, the tips were washed with chloroform and dried with N_2 gas. The tips were incubated for 2.5 hours in 100 µL LDL (0.06 mg/mL in PBS), to which 2 µL $NaCNBH_3$ (1 M, freshly prepared in 10 mM NaOH) was added for irreversible binding. Afterwards, 5 µL of ethanolamine hydrochloride (1 M, adjusted to pH 9.6) was added for blocking non-reacted linker groups and incubation was continued for 10 min. This chemical modification was used to covalently link fluorescent lipoprotein particles on cantilevers.

Preparation of planar Supported Lipid Bilayers (SLB): Glass slides (d = 22 mm, Menzel) were incubated in a freshly prepared mixture of concentrated sulfuric acid : hydrogen peroxide (3 : 1) for 20 min, rinsed with deionized water and ethanol and dried under nitrogen flow as previously described [5,6]. Glass slides were then mounted onto the sample plate of the combined force and fluorescence microscope. 30 µL of DOPC solution (10 mg/mL in chloroform : methanol (3 : 1)) was evaporated under nitrogen (20 min) and resuspended in 300 µL of PBS. For experiments on pre-inserted fluorescent lipids, we mixed the DOPC lipids with low concentrations of C-BodipyFL before the evaporation step. Vesicles were prepared by ultra-sonication for 20 min and applied to the sample surface. SLB were formed on mica (for HS-AFM experiments) or on glass surfaces (for combined force/fluorescence- and for fluorescence microscopy only). Mica was freshly cleaved before usage. The bilayer had formed after 20 min, and the chamber was washed with PBS. For high-speed AFM measurements, only 1/10 of the incubation volume with the same lipid concentration was used.

Preparation of Giant Unilamellar Vesicles (GUVs): GUVs were prepared by electroformation at room temperature [7,8]. This technique produces vesicles with varying sizes from 10 µm to 100 µm. DOPC was dissolved in chloroform/methanol (10 mg/mL) and deposited on Pt electrodes and the solvent was evaporated by a constant N_2 flow for 20min. 300 µL of 100 mM sucrose solution was added in a home-made chamber that allows visualization in the microscope. We placed in the chamber cap two holes with a distance of 5 mm for the electrodes. After the electrodes with dried lipids were submerged into the sugar solution, a voltage of 1.1 V at 10 Hz for 1 h and for another 30 min a voltage of 2.1 V at 2 Hz was applied. For imaging, we added 300 µL of a 150 mM glucose solution. Fluorescently labeled LDL particle solution was added to the suspension containing the GUVs (final lipoprotein particle concentration 0.3 mg/mL). Images were acquired 20 min after lipoprotein addition by confocal microscopy.

Preparation of Giant Plasma Membrane Vesicles (GPMVs): CHOK1 cells were seeded in cell culture dishes until reaching 70% confluency and GPMVs were formed as described by Baumgart et.al [9]. Briefly, cells were washed twice with 1 ml GPMV buffer (10 mM HEPES, 150 mM NaCl, 2 mM $CaCl_2$, pH 7.4). 1 mL of GPMV buffer was added to the cells. 18 µL of 4% para-Formaldehyde was added to the supernatant solution of the culture dish (final concentration 25 µM). Immediately afterwards, 20 µL of 1 M dithiothreitol solution was added (final concentration = 20 mM). Cells were incubated at 37 °C for 1 h. After formation, GPMVs were

separated from vesiculation agents by differential centrifugation. Partitioning was measured with confocal microscopy and membrane order was quantified by C-Laurdan microscopy. Afterwards, purified GPMVs were incubated with fluorescently tagged lipoproteins for 10 min at 4 °C.

FCS and FCCS experiments: Vesicles were incubated in glass bottom Ibidi chambers (# 1.5) for 15 minutes for precipitation. Fluorescence Correlation Spectroscopy (FCS) and Fluorescence Cross-Correlation Spectroscopy (FCCS) measurements were done on the bottom membrane of GUVs using an Abberior Resolft Microscopy system (Oil immersion objective 100x NA 1.4, APD detectors, 488 nm and 640 nm excitation lasers) or Zeiss 780 LSM system (water immersion objective 40x NA 1.2, GaAsP detectors, 488 nm and 633 nm excitation lasers). For Abberior system, the detectors were connected to a correlator card (correlator.com) which was controlled by Flex program. Three measurements (10 seconds each) were done on each vesicle. At least, five vesicles were measured per sample. For FCCS measurements, the system is calibrated using Alexa488 and Alexa647 dyes. The imperfect cross-correlation stems from the relatively different sizes of the green and red excitation beams.

Obtained auto- and cross-correlation curves were fitted with a 2D- or 3D-diffusion plus triplet model [10], for membrane and solution measurements, respectively. The models are described below.

For 3D: $G(\tau)_{3D} = \frac{1}{N}\left(1+\frac{\tau}{\tau_D}\right)^{-1}\frac{1}{\sqrt{(1+\omega^2\frac{\tau}{\tau_D}}}$

For 2D: $G(\tau)_{2D} = \frac{1}{N}\left(1+\frac{\tau}{\tau_D}\right)^{-1}$

For 2D + Triplet : $G(\tau)_{2D+T} = G(\tau)_{2D}\left[1+T(1-T)^{-1}\exp(\frac{-\tau}{\tau_{Tr}})\right]$

For 3D + Triplet : $G(\tau)_{3D+T} = G(\tau)_{3D}\left[1+T(1-T)^{-1}\exp(\frac{-\tau}{\tau_{Tr}})\right]$

For fitting, FoCuS-point software is used [11].

C-Laurdan Microscopy. For GP determination, vesicles were doped with 0.4 µM C-Laurdan and imaged with a BioRad two-photon microscope. An 800 nm laser was used for excitation. Emission was collected in two channels, 440 nm and 490 nm constituting the ordered and disordered channels, respectively. GP values were calculated by division of the difference between the ordered and disordered channels and their sum [12].

High-speed AFM: High-speed AFM was used as developed by the group of T. Ando [13,14]. It was operated in tapping mode at room temperature (25 °C) with free amplitudes of 1.5 nm - 2.5 nm and a set point of larger than 90% of the free amplitude. For this study, we used USC-F1.2-k0.15

cantilevers (NanoWorld AG, Switzerland) with nominal spring constants of ~150 pN/nm, a resonance frequency of ~500 kHz, and a quality factor of ~2 in liquids. For imaging single lipoprotein particles on mica, the sample (LDL particle) was diluted in PBS buffer (~1:500), incubated for 5 min on freshly cleaved mica, rinsed and imaged in PBS. For the observation of the interaction of lipoproteins with a membrane, a supported lipid (DOPC) bilayer was formed on mica (as described above). After rinsing the sample with PBS, lipoprotein particles (again diluted ~1:500 in PBS) were injected while imaging. High-speed AFM images were processed and analyzed in Gwyddion 2.49 (CMI, Czech Republic). Statistical analysis of particle heights was performed using MATLAB (Mathworks, MA, USA). Probability density functions (pdfs) representing the distribution of particle heights were calculated using the ksdensity function in MATLAB.

Combined Single Molecule Fluorescence and Force Microscopy: A tip-scanning PicoPlus AFM (Agilent Technologies, Chandler, AZ) was mounted on the fluorescence microscope via a home-built plate on a high-precision XY-stage (Scan IM 120 x100, Märzhäuser). The cantilever was first aligned with the optical axis via the XY-stage, and the sample region of interest was then positioned to the field of view of the camera via x-y screws on the AFM head. The combined microscope was placed on a passive anti-vibration table without additional active damping (Newport). AFM force spectroscopy was performed using silicon cantilevers with a nominal spring constant of 0.01 N/m or 0.02 N/m (Veeco). The two instruments were synchronized via TTL signals: the AFM was used as master, which triggered predefined imaging protocols on the fluorescence microscope. Typically, we started an experiment by parking the AFM tip at a predetermined distance from the surface (~3 µm). The start of the approach curve was used to trigger the illumination protocol; this allowed for optically monitoring the approach, hold, and retraction part. TIR excitation ensured that the tip was only illuminated during the short time period when it came into proximity of the bilayer, thereby limiting photobleaching. The illumination time for individual images was 5 ms. Silicon-nitride AFM cantilevers with silicon tips (MSNL-10) were amine-functionalized as described above and modified with lipoprotein particles.

Confocal Imaging:

GUVs and GPMVs were imaged with a laser scanning confocal microscope (LSM 700 AxioObserver, Zeiss). The microscope was equipped with a Plan-Apochromat 63x/1.40 Oil DIC M27 objective (Zeiss). The LSM 700 operates with solid-lasers (polarization-preserving single-

mode fibers) at a wavelength of 639 nm and 488 nm. Signals were detected after appropriate filtering on a photomultiplier. Typically, z-stacks were done with a step size of 500 nm. Detector amplification, laser power and pinhole were kept constant for all measurements. Images were analyzed by thresholding the C-BodipyFL signal; the average pixel value of signals underneath the obtained mask was calculated in both the C-BodipyFL and the protein-Atto647N channel. For each experiment at least 10 GUVs and GPMVs were evaluated. Partition coefficients were determined as previously reported [15].

Cells were grown until just reaching confluency in individual LabTek™ chambers (8 chambers per slide, each 4 mm x 4 mm surface area, ~700 µl total volume, Thermo Fisher Scientific), washed once with pre-warmed HBSS and incubated with fluorescently labeled LDL solution (incubation concentration 5 µg/mL) for 15 min at different temperatures (4 °C, 12 °C, 18 °C and 37 °C) in the dark. Samples were washed thrice with ice-cold PBS and cells were fixed using a 4% PFA solution. Phase-contrast and confocal fluorescence images were obtained using an Olympus imaging device (Fv10i) equipped with an UPLSAP60xW objective (NA=1.2) at two fluorescence detection channels (excitation at 499 nm and 653 nm with detection at 520 nm and 668 nm, respectively). Pinhole was maximal opened to achieve a maximal depth of field. Experiments were performed in PBS at room temperature. Individual cells were identified via their phase contrast image manually and the average fluorescence intensity in the corresponding fluorescence images was calculated, background-corrected (background value was obtained in areas without cells) and corrected for cellular auto-fluorescence (negative control experiment with addition of solely unlabeled LDL).

Single Molecule/Particle Tracking: For the analysis of fluorescence images, individual diffraction limited signals were selected, fitted with a Gaussian intensity profile, and tracked using in-house algorithms implemented in MATLAB (MathWorks); the single molecule positions were obtained to an accuracy of σ_{xy} = 20 nm – 40 nm. In case of AFM images, topographical profiles were analyzed by cross-section profiling (we used the free software Gwyddion, and scanning and analysis software kindly provided by Toshio Ando). Individual particles were identified and fitted with a Gaussian profile, yielding the position to an accuracy of σ_{xy} = 2 nm. For single particle tracking, AFM images were analyzed using ImageJ. Single molecule/particle diffusion constants were determined as described previously [16]. In brief, trajectories are characterized by a sequence of positions $\vec{x}(i)$, with i ranging from 1 to the number of observations of this trajectory. The mean

square displacements $\langle r^2 \rangle$ were calculated as a function of the time-lag $t_{lag} = n(t_{ill} + t_{delay})$ according to

$$\langle r^2 \rangle = \langle \left(\vec{x}(i) - \vec{x}(n+i) \right)^2 \rangle_{i=1;1+n,1+2n;\dots} \quad (1)$$

with n denoting the difference in frame index.

Data were analyzed by fitting with:

$$\langle r^2 \rangle = 4Dt_{lag} + 4\sigma_{xy}^2 \quad (2)$$

yielding the lateral diffusion constant D and the single molecule localization precision σ_{xy}.

The density of transferred molecules upon contact of the LDL-coated tip with the bilayer was too high for single molecule tracking. We thus opted for a different strategy for estimating the diffusion constant by fitting the time-dependent dispersion of the fluorescence signal from the central source. The center of the Gaussian distribution (x_0, y_0) was estimated by finding the coordinates of the brightest pixel in the image. The probability density function for 2-dimensional diffusion is given by

$$f(x,y) \cdot dx \cdot dy = \frac{1}{4\pi \cdot D \cdot t} \cdot e^{\left[-\frac{(x-x_0)^2}{4 \cdot D \cdot t} - \frac{(y-y_0)^2}{4 \cdot D \cdot t} \right]} \cdot dx \cdot dy$$

and characterized by a variance:

$$Var = \int_{-\infty}^{+\infty} \int_{-\infty}^{+\infty} [(x-x_0)^2 + (y-y_0)^2] \cdot f(x,y) \cdot dx \cdot dy = 4 \cdot D \cdot t$$

By choosing a window of appropriate size around the maximum the variance was calculated by the following equation:

$$Var = \frac{\sum_{x,y} [I(x,y) - b][(x-x_0)^2 + (y-y_0)^2]}{\sum_{x,y} [I(x,y) - b]}$$

with (x,y) the coordinate of the respective pixel inside the estimation window, I(x,y) the brightness of the corresponding pixel and b an estimation of the overall background. b was determined by calculating the mean brightness of a five pixel ring around the estimation windows. Due to the diffusion process the 2D Gaussian function broadens over time depending on the time lag between two consecutive images and the diffusion constant. To ensure fair parameter estimation the window size was increased by several pixels for each subsequent image. Variances versus time were fit according to:

$$Var = 4Dt + const \quad (3)$$

where the constant term accounts for the resolution of the microscope.

SUPPORTING FIGURES

Supplementary Figure 1 | LDL particle interaction with GUVs and subsequent C-BodipyFL transfer.

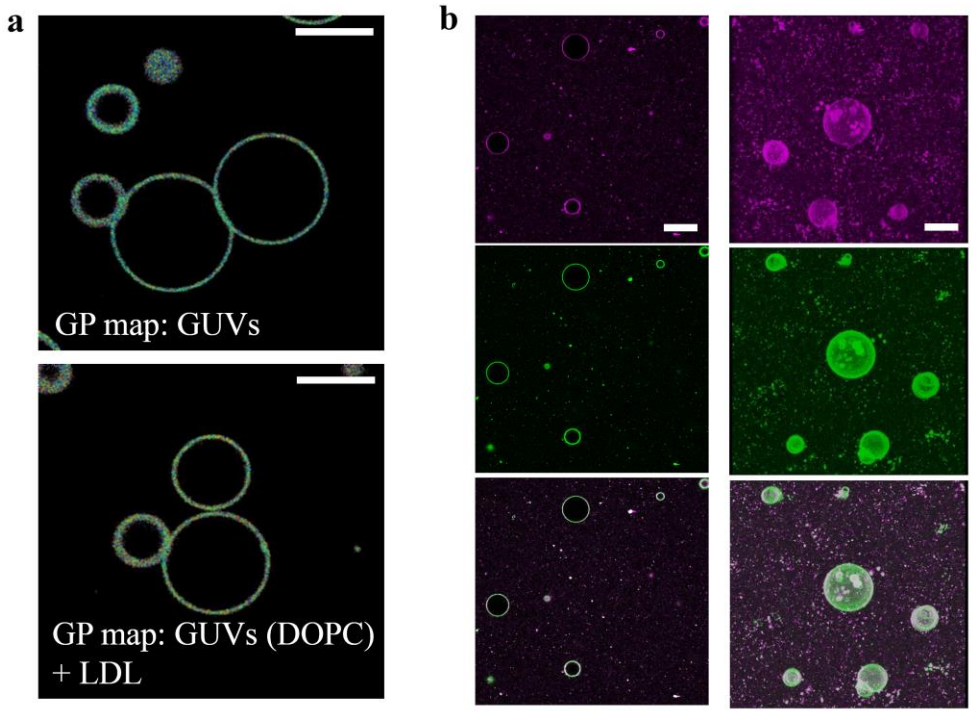

(a) GUVs were prepared using DOPC with 0.01 mol% C-Laurdan. Fluorescently labeled LDL particles were added for 2 minutes and subsequently visualized. The quantitative analysis of the average C-BodipyFL and protein-Atto647N signal as a function of the GP values obtained for GUVs alone and GUVs incubated with LDL particles is provided in Figure 2a. Here, representative raw data is visualized. Scale bar = 10 µm (b) The individual signal of protein-Atto647N (upper row), C-BodipyFL (middle row) and the corresponding overlay (lower row) was imaged as a snap shot from a certain z-range (left row) and three-dimensional (right row) stack. Scale bar = 20 µm. Measurements were performed at room temperature.

Supplementary Figure 2 | Topography of lipoprotein particles on planar supported membranes and mica. Temporal LDL particle transfer/interaction with planar supported membranes.

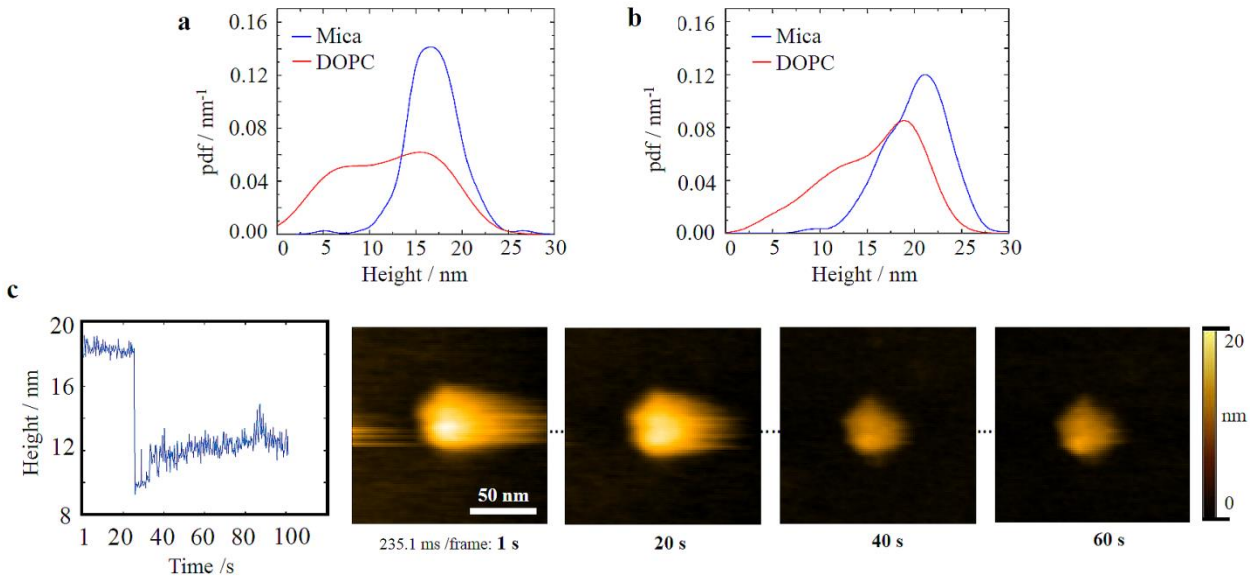

LDL particles from three different healthy subjects were investigated using HS-AFM. The height distributions of LDL particles from donor 1 are shown in Figure 4c. (a) pdf of particle heights on mica and supported DOPC-bilayers of samples from donor 2 (mica: N = 145, DOPC: N = 129) and (b) donor 3 (mica: N = 403, DOPC: N = 213). (c) HS-AFM imaging temporally resolves the interaction of LDL particles with the DOPC membrane. The time trace of particle height (left) and the corresponding topography images (right) demonstrate the fusion of LDL particles with the membrane. Measurements were performed in PBS at room temperature.

Supplementary Figure 3 | Specific interaction and fusion of LDL particles with LUVs.

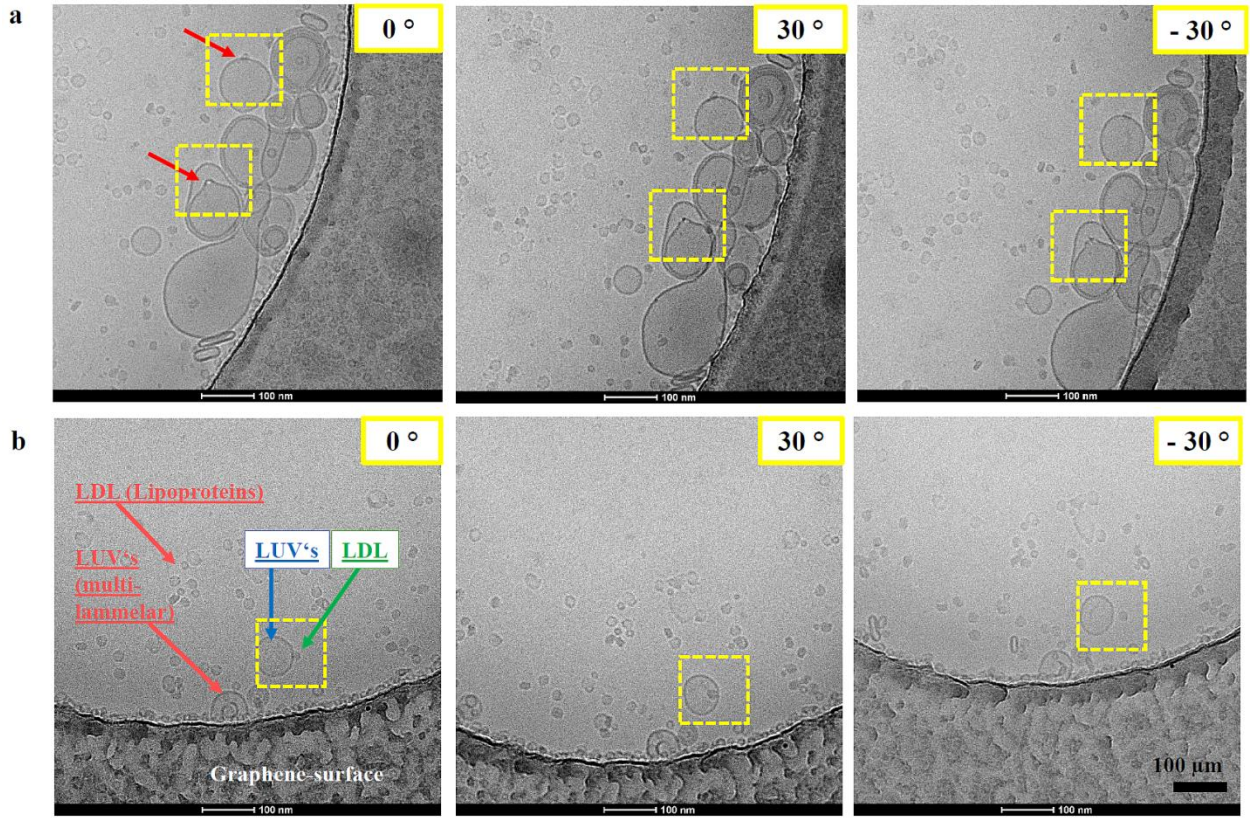

(a) LDL particle incorporation into the LUV membrane (red arrow and yellow boxes) was confirmed through recording data under different electron-beam incident angles. To discriminate between an accidental overlay of signals originating from different layers of the vitrified ice (exemplified in the yellow-dotted box), various imaging angles were recorded (left 0°, middle 30°, right -30°). In this particular case, only a single-angle image would lead to a wrong data interpretation. (b) Cryo-EM images of LDL particles (green arrow) on decorated LUVs (blue arrow) were obtained at specified angle settings. Owing to their different size and morphology, LUVs and LDL particles can be clearly distinguished in cryo-EM images. Images were acquired under low-dose conditions (*20 e^-/Å*).

Supplementary Movie 1 | Combined approach AFM/SMFM

Supplementary Movie 2 | Temporal interaction of LDL particles / HS-AFM

REFERENCES

(1) Kim, H. M.; Choo, H.; Jung, S.; Ko, Y. A Two-Photon Fluorescent Probe for Lipid Raft Imaging : C-Laurdan. *ChemBioChem* **2007**, *8*, 553–559.

(2) Schumaker, V. N.; Puppione, D. L. Sequential Flotation Ultracentrifugation. *Methods Enzymol.* **1986**, *128* (C), 155–170.

(3) Ebner, A.; Hinterdorfer, P.; Gruber, H. J. Comparison of Different Aminofunctionalization Strategies for Attachment of Single Antibodies to AFM Cantilevers. *Ultramicroscopy 107* **2007**, *107*, 922–927.

(4) Wildling, L.; Unterauer, B.; Zhu, R.; Rupprecht, A.; Haselgr, T.; Rankl, C.; Ebner, A.; Vater, D.; Pollheimer, P.; Pohl, E. E.; et al. Linking of Sensor Molecules with Amino Groups to Amino-Functionalized AFM Tips. *Bioconjugate Chem* **2011**, *22*, 1239–1248.

(5) Plochberger, B.; Stockner, T.; Chiantia, S.; Brameshuber, M.; Weghuber, J.; Hermetter, A.; Schwille, P.; Schütz, G. J. Cholesterol Slows down the Lateral Mobility of an Oxidized Phospholipid in a Supported Lipid Bilayer. *Langmuir* **2010**, *26* (22), 17322–17329.

(6) Axmann, M.; Schütz, G. J.; Huppa, J. B. Single Molecule Fluorescence Microscopy on Planar Supported Bilayers. *J. Vis. Exp.* **2015**, *2015* (104), 53158.

(7) Montes, L. R.; Alonso, A.; Goñi, F. M.; Bagatolli, L. A. Giant Unilamellar Vesicles Electroformed from Native Membranes and Organic Lipid Mixtures under Physiological Conditions. *Biophys. J.* **2007**, *93* (10), 3548–3554.

(8) Girard, P.; Pécréaux, J.; Lenoir, G.; Falson, P.; Rigaud, J.-L.; Bassereau, P. A New Method for the Reconstitution of Membrane Proteins into Giant Unilamellar Vesicles. *Biophys. J.*

2004, *87* (1), 419–429.

(9) Baumgart, T.; Hammond, A. T.; Sengupta, P.; Hess, S. T.; Holowka, D. A.; Baird, B. A.; Webb, W. W. Large-Scale Fluid/Fluid Phase Separation of Proteins and Lipids in Giant Plasma Membrane Vesicles. *Proc. Natl. Acad. Sci.* **2007**, *104* (9), 3165–3170.

(10) Sezgin, E.; Schwille, P. Fluorescence Techniques to Study Lipid Dynamics. *Perspect Biol* **2011**, *3*, 1–32.

(11) Waithe, D.; Clausen, M. P.; Sezgin, E.; Eggeling, C. FoCuS-Point : Software for STED Fluorescence Correlation and Time-Gated Single Photon Counting. *Bioinformatics* **2016**, *32* (6), 958–960.

(12) Sezgin, E.; Levental, I.; Grzybek, M.; Schwarzmann, G.; Mueller, V.; Honigmann, A.; Belov, V. N.; Eggeling, C.; Coskun, Ü.; Simons, K.; et al. Partitioning , Diffusion , and Ligand Binding of Raft Lipid Analogs in Model and Cellular Plasma Membranes. *BBA - Biomembr.* **2012**, *1818* (7), 1777–1784.

(13) Ando, T.; Uchihashi, T.; Fukuma, T. High-Speed Atomic Force Microscopy for Nano-Visualization of Dynamic Biomolecular Processes. *Prog. Surf. Sci.* **2008**, *83* (7–9), 337–437.

(14) Review, T. High-Speed Atomic Force Microscopy Coming of Age. *Nanotechnology* **2012**, *23* (6).

(15) Baumgart, T.; Hunt, G.; Farkas, E. R.; Webb, W. W.; Gerald, W. Fluorescence Probe Partitioning between Lo/Ld Phases in Lipidmembranes. *Biochim Biophys Acta* **2009**, *1768* (9), 2182–2194.

(16) Wieser, S.; Schütz, G. J. Tracking Single Molecules in the Live Cell Plasma Membrane-Do's and Don't's. *Methods* **2008**, *46* (2), 131–140.